2006

Predication of multi-dimensional photonic crystal structures generated by multi-beam interference in holographic lithography

Jose F. Chicharo
University of Wollongong, chicharo@uow.edu.au

Jiangtao Xi
University of Wollongong, jiangtao@uow.edu.au

Enbang Li
University of Wollongong, enbang@uow.edu.au

Publication Details

Li, E., Xi, J. Chicharo, J. F. (2006). Predication of multi-dimensional photonic crystal structures generated by multi-beam interference in holographic lithography. Smart Materials and Structures, 15 (1), S158-S164. >

Predication of multi-dimensional photonic crystal structures generated by multi-beam interference in holographic lithography

Enbang Li, Jiangtao Xi and Joe Chicharo
School of Electrical, Computer and Telecommunications Engineering
Faculty of Informatics
University of Wollongong

ABSTRACT

Photonic crystals (PCs) are synthetic micro-structures which have periodical refraction index variations and produce photonic band gaps similar to electronic band gaps produced by the crystal potentials of semiconductors. Different methods have been proposed and demonstrated to fabricate two- or three-dimensional photonic crystal structures. Among them, the holographic lithography method, in which multi-beam interference is employed, offers a number of advantages, including its ability to create large volume of periodic structures through an irradiation process, the uniformity of period, and more degrees of freedom to control the structures. In this study, a multi-beam interference model is presented for predicting the mulit-dimensional photonic crystal structures. Various parameters, including beam propagation and polarization directions, beam intensities, and phase shifts are considered. Calculations have been carried out to simulate two four-beam configurations which have been popularly used in the fabrication of photonic crystals. It has been demonstrated that the contours of the interference pattern are related to the polarization states, the intensity ratios among the four beams, and the phase delays. Therefore, by controlling the beam intensities, polarization directions, and phase delays, different structures can be obtained. The results presented in this study provide a useful guide for choosing various optical parameters and selecting proper photoresists to fabricate 2D and 3D photonic crystal structures.

Keywords: photonic crystal, holographic lithography, laser beam, interference

1. INTRODUCTION

Photonic crystals (PCs), also known as phonotic band gap (PBG) materials, are synthetic micro-structures which have periodical refraction index variations.[1, 2] In recent years, intensive research efforts have been devoted to the studies of photonic crystals due to their possibility to manipulate and control light.[3-5] Many promising applications such as high-density integrated optical circuits and thresholdless lasers are currently under investigation and development.[6] The research on photonic crystals is not only creating new devices for telecommunications applications, but also opening a new area in fundamental studies. Although different methods have been demonstrated to fabricate photonic crystals, it is still a challenging task to make a photonic crystal with complete 3D bandgaps, especially in the near-infrared or visible band. Method based on the semiconductor fabrication technology, which includes lithography, layering, and etching processes, has been widely used.[7-10] One of the obvious advantages of using semiconductor materials is the high dielectric contrast, which is critical for providing a complete band gap. However, this method requires expensive and large-scale equipment. Laser microfabrication, which uses visible or ultraviolet laser-induced polymerization, has also been demonstrated to make photonic crystals.[11] By using laser microfabrication, arbitrary structures could be fabricated and the optical properties of the structures could be tailored. More recently, methods based on holographic lithography and photo-induced polymerization have been proposed and demonstrated.[12-16] With these methods, a film of photoresist is first exposed to an interference pattern generated by multiple laser beams. After development, the unexposed areas (for a negative-tone photoresist) are dissolved away hence a periodic structure with air-filled voids is formed. This structure can be directly used as a photonic crystal, or as a template for infiltration of other materials with high dielectric constants. Compared with the conventional semiconductor and micro-machining techniques, the holographic lithography method has a number of advantages, including its ability to create large volume of periodic structures through an irradiation process, the uniformity of period, and more degrees of freedom to control the structures.

In this study, a multi-beam interference model is presented for predicting 2D and 3Dt photonic crystal structures. Various parameters, including beam propagation and polarization directions, beam intensities, and phase shifts are considered. Calculations have been carried out to simulate a four-beam configuration to generate three-dimensional structures. It has been demonstrated that by controlling the beam intensities and polarization directions, different structures can be obtained. The results provide a useful guide for choosing various optical parameters and selecting proper photoresists to fabricate three-dimensional photonic crystals.

2. MULTI-BEAM INTERFERENCE MODEL

In order to analyze 2D and 3D fringe patterns generated by the multi-beam interference, we first present here a general expression of a laser beam, which describes its propagation direction, polarization state, wave front shape, and phase delay.

The electrical field distribution of a laser beam propagating along the z-axis can be generally described by

$$\vec{E}(x,y,z) = [\vec{e}_x E_x + \vec{e}_y E_y \exp\{i\delta\}]E(x,y)\exp\{i(kz + \Phi(x,y,z))\} \tag{1}$$

where, $\vec{e}_x$ and $\vec{e}_y$ are unit vectors along the x- and y-axis respectively; E_x and E_y are the amplitudes in the x and y directions.

In Eq.(1), δ is a phase delay, it represents different polarization states of the laser beam: $\delta = m\pi (m = 0, \pm 1, \pm 2, \cdots)$ indicates that the beam is linearly polarized, while $\delta = \pm \pi / 2$ and $E_x = E_y$ means that the polarization of the light is circular. For a more general case, the polarization of the light is elliptical.

$E(x, y)$ in Eq.(1) represents the amplitude variations in the x-y plane. When the laser operates in its fundamental mode, ie TEM_{00} mode, $E(x, y)$ has a Gaussian distribution.

In Eq.(1), $\Phi(x, y, z)$ is a function describing the wave front of the laser beam. For a Gaussian beam, we have

$$\Phi(x, y, z) = \Phi_0 + k\frac{x^2 + y^2}{2R(z)} - \tan^{-1}(z / z_0) \qquad (2)$$

where,

$z_0 = \pi w_0^2 / \lambda$,

$R(z) = z[1 + (z_0 / z)^2]^{1/2}$,

w_0 is the beam waist radius of the laser beam, and Φ_0 is the initial phase. In a multi-beam interference situation, Φ_0 describes any possible phase delays caused by different optical paths.

For a plane wave, $E(x, y)$ = constant, and $\Phi(x, y, z) = \Phi_0$. Although real plane waves do not exist, in some applications, the plane wave model does give a good approximation to the real laser beam and significantly simplifies the process. In some situations, for instance, when the laser beam is sharply focused, the Gaussian beam model has to be used. In this study, we will present a multi-beam model based on the plane wave assumption.

In order to generate three-dimensional interference structures, at least three coherent laser beams have to be used. Therefore, the interference pattern generated by multiple coherent laser beams needs to be investigated. From Eq.(1), we can write the *n*th individual beam propagating in a local x_n-y_n-z_n coordinate system as

$$\vec{E}_n(x_n, y_n, z_n) = [\vec{e}_{xn}E_{xn} + \vec{e}_{yn}E_{yn}\exp\{i\delta_n\}]\exp\{i(kz_n + \Phi_{0n})\}, \qquad n = 1,2,\cdots \tag{3}$$

We consider N beams intersecting at the origin of a global x-y-z coordinate system. The total field vector is given by

$$\vec{E}(x, y, z) = \sum_{n=1}^{N}[\vec{e}_{xn}E_{xn} + \vec{e}_{yn}E_{yn}\exp\{i\delta_n\}]\exp\{i(kz_n + \Phi_{0n})\} \quad . \tag{4}$$

It should be noted that the sum operation in Eq.(4) is carried out among all field vectors of the incident beams.

The intensity distribution produced by the interference of the N beams can be expressed as

$$I(x, y, z) = \vec{E}(x, y, z) \bullet \vec{E}(x, y, z)^*, \tag{5}$$

where, $\vec{E}(x, y, z)^*$ denotes the conjugate of $\vec{E}(x, y, z)$.

The coordinates and polarization directions of the individual beams can be transformed to the global coordinates by using the following transformations:

$$\begin{aligned} x_n &= x\cos\alpha_{n1} + y\cos\beta_{n1} + z\cos\gamma_{n1} \\ y_n &= x\cos\alpha_{n2} + y\cos\beta_{n2} + z\cos\gamma_{n2} \\ z_n &= x\cos\alpha_{n3} + y\cos\beta_{n3} + z\cos\gamma_{n3} \end{aligned} \quad , \tag{6}$$

where, α_{nm}, β_{nm}, γ_{nm} (m = 1, 2, 3) are respectively the orientation angles of the x_n-, y_n- and z_n-axis in the global coordinate system. If we consider a simple situation where the x_n-y_n-z_n coordinate system is a transformation by first rotating the global coordinate system around the z-axis by θ and then rotating around the x-axis by φ, as shown in Fig.1, then Eq.(6) can be simplified as

$$
\begin{aligned}
x_n &= x\cos\theta + y\sin\theta \\
y_n &= -x\cos\varphi\sin\theta + y\cos\varphi\cos\theta + z\sin\varphi \quad . \\
z_n &= x\sin\varphi\sin\theta - y\sin\varphi\cos\theta + z\cos\varphi
\end{aligned} \tag{7}
$$

The interference intensity distribution in the global coordinate system can be predicted by using Eqs.(2-7) if the orientations and polarizations of the incident beams are known. With the knowledge of the photosensitivity and threshold of the photoresists, which are exposed to the interference patterns, the structures of the photonic crystals can be predicted. In the next section, as examples we use the multi-beam model to calculate photonic crystal structures generated by a four beam configuration and present the results with different polarization directions and exposures.

3. MULTI-DIMENSIONAL PHOTONIC CRYSTAL STRUCTURES

Using the multi-beam interference model presented in previous section, we calculated different 2D and 3D interference structures which are of interest to the photonic crystal fabrications. In the simulations, the wavelength of the laser beams was chosen as 355 nm, which can be generated from the third-harmonic of a YAG laser and has been used in the fabrication of 2D and3D photonic crystals.

3.1 2D SQUARE STRUCTURES

A 2D square periodic structure can be generated by using a four-beam arrangement shown in Fig.2. Four laser beams (B1, B2, B3, and B4) are split from a single beam by using either beam splitters or a diffraction grating, and symmetrically arranged around the z-axis. B1 and B2 are in the x-z plane, and B3 and B4 are in the y-z plane.

Shown in Fig.3 is the intensity distribution produced by the interference of four beams. All of the incident beams linearly polarize in the x-z plane and there is no phase delay among them. As expected, a periodic square structure is formed, and the structure does not vary along the z-axis meaning that the square structure is two-dimensional. In order to examine the influence of the polarization states of the incident beams on the interference patterns, we calculated the intensity distributions under different combinations of polarization directions. Depicted in Fig.4 is a calculated result for a situation where the directions of polarizations of B3 and B4 are in the y-z plane. Interestingly the period and the orientation of the structure are completely different from that shown in Fig.3. We note that this structure seems to be generated by adding a peak in the center of every square in Fig.3. In fact, since the two pairs of interference beams, (B1, B2) and (B3, B4) are polarizing in two orthogonal planes, the interferences only happen between B1 and B2, and between B3 and B4 independently. The structure shown in Fig.4 is actually a superposition of two sets of one-dimensional patterns produced by the interferences of B1 and B2, and B3 and B4 respectively. Another situation we considered is that all beams are circularly polarized. In this case, a structure similar to that shown in Fig.4 is produced.

We further examined the affect of phase delays among the incident beams. Our calculated results show that when the incident beams linearly polarize in the x-z plane, by introducing a phase delay in any beam from 0 to π, the produced structure will change gradually from the one as shown in Fig.3 to that as shown in Fig.4. Similar results have been previously reported in Ref. 13.

3.2 3D STRUCTURES

3D photonic crystal structures can also be generated by a four-beam interference. Rearranging the laser beams (B1, B2, B3, and B4) shown in Fig.2, we have a configuration as shown in

Fig.5. This configuration has been used in fabricating 3D photonic crystals in Ref. 12, 15 and 16. Referring to Fig.5, B4 propagates along the z-axis, and B1, B2, and B3 are symmetrically arranged around B4 and have an angle of φ with B4. The incidence plane of B1 is the y-z plane. In the current simulations, we assumed that the incident beams are plane waves, however, as we indicate in the previous section, the model introduced in this study can be used for other light waves, such as fundamental and high order Gaussian beams.

We first considered a situation where B1, B2 and B3 have the same intensity, and linearly polarize in their incidence planes respectively. B4 has an intensity twice of other beams and is circularly polarized. In the simulation, the incident angle of B1, B2 and B3, φ, was set as 38.9 degrees.

Shown in Fig.6 is a contour plot of the intensity distribution in the x-y plane at z=0. The four-beam configuration shown in Fig.5 generates an interference pattern of 3D periodic structures with face-centered cubic (fcc) symmetry. The x-y plane corresponds the (111) plane of the fcc structure. When a film of photoresist is exposed to the interference pattern and processed, a 3D structure corresponding to the interference pattern is formed in the film. Shown in Fig.7 is a structure formed when a photoresist exposed to the pattern shown in Fig.6. The dark color indicates the air voids after the photoresist is developed. In the calculation, we assumed that the total exposure (sum of the energy densities of four beams) exceeds 1.5 times of the threshold of the photoresist. We chose to use the total exposure as a control parameter because it can be directly measured and adjusted in the experiments. From Fig.6 and Fig.7, it can be seen that the contours of the intensity distributions in the x-y plane are not circular but triangular. The interference patterns in the x-z plane (y=0) and the y-z plane (x=0) are shown in

Fig.8 and Fig.9 respectively.

With the current model, we can also calculate the filling fraction of the formed photonic crystals. Fig.10 is the calculated filling fractions at different exposure dosages which are normalized by the threshold of the photoresist. The filling fraction almost linearly increases with the exposure and gradually saturates when the total exposure exceeds the threshold of the photoresist. With the knowledge of the photoresist characteristics, one can determine the total exposure needed to achieve the desired filling fraction. It should be pointed out that the relationship between the filling fraction and the exposure is dependent on the intensity ratios among the incident beams and their polarization directions.

In order to examine the influence of the beam polarization, we changed the states of polarizations of B1, B2 and B3 from linear to circular and calculated the interference intensities at different positions along the z-axis. The results are shown in Fig.11. For the comparison purpose, we also present in Fig.12 the intensity distributions of the situation where B1, B2 and B3 are linearly polarized.

When the intensity ratios among the four beams are varied, the interference patterns could change dramatically. For the case where all the four beams are circularly polarized, for instance, when the intensity of B4 is reduced to half of that of other beams, interference patterns as shown in Fig.13 were obtained. Compared with Fig.11, we can find that besides the structure features shown in Fig.11, another structure with smaller lattice spacing appears. This is because that the interference among B1, B2 and B3 will become obvious when the intensity of B4 is reduced. Another difference is that the intensity contours are of circular shapes, comparing with the triangular contours shown in Fig.11 and Fig.12.

4. CONCLUSIONS

In this study, we introduce a multi-beam interference model for predicting the multi -dimensional periodic structures used for photonic crystal fabrication. All beam parameters including propagation direction, polarization states and directions, and phase shifts caused by optical path delay have been taken into account in the proposed model. Calculations were carried out to simulate two four-beam configurations which have been popularly used in the fabrication of photonic crystals. In particular, we calculated the 2D square structures produced by the four-beam interference configuration shown in Fig. 2. We found that the polarization directions of the incident beams and the phase delays among the beams play important roles in the interference.

We also simulated a configuration for producing 3D periodic structures. Two situations were considered: (1) the central beam is circularly polarized and the others are linearly polarized in their incidence planes; (2) all the beams are circularly polarized. Our simulations demonstrate that the contours of the interference pattern are related to the polarization states and the intensity ratios among the four beams. For instance, when all of the incident beams are circularly polarized, the contours of the interference pattern are close to circular shapes. This means that one can control the shapes of the air-filled voids of a photonic crystal by adjusting the parameters of the incident beams. With the current model, we also calculated the fill fractions of the 3D structures under different exposures.

The results presented in this study provide a useful guide for choosing various optical parameters and selecting proper photoresist to fabricate three-dimensional photonic crystals by using the holographic lithography method.

REFERENCES

1. E. Yablonovitch, "Photonic band-gap structures," *Journal of Optical Society of America B*, **Vol.** 10, 283-295, 1993.
2. H. S. Sozuer and J. W. Haus, " Photonic bands: simple-cubic lattice," *Journal of Optical Society of America B*, **Vol. 10**, 296-302, 1993.
3. S. Y. Lin, E. Chow, V. Hietala, P. R. Villeneuve and J. D. Joannopoulos, "Experimental demonstration of guiding and bending of electromagnetic waves in a photonic crystal," *Science*, **Vol.** 282, 274-276, 1998.
4. L. C. Andreani and M. Agio, "Photonic bands and gap maps in a photonic crystal slab," *IEEE Journal of Quantum Electronics*, **Vol.** 38, 891-898, 2002.
5. Z.-Y. Li, I. El-Kady and K.-M. Ho, "Photonic band gap effect in layer-by-layer metallic photonic crystals," *Journal of Applied Physics*, **Vol.** 93, 38-42, 2003.
6. A. Chutinan and S. Noda, "Highly confined waveguides and waveguide bends in three-dimensional photonic crystal," *Applied Physics Letters*, **Vol.** 75, 3739-3741, 1999.
7. J. Schilling, F. Muller, S. Matthias, R. B. Wehrspohn and U. Gosele, "Three-dimensional photonic crystals based on macroporous silicon with modulated pore diameter," *Applied Physics Letters*, **Vol.** 78, 1180-1182, 2001.
8. A. Talneau, L. Le Gouezigou, N. Bouadma, M. Kafesaki, C. M. Soukoulis and M. Agio, "Photonic-crystal ultrashort bends with improved transmission and low reflection at 1.55 μm," *Applied Physics Letters*, **Vol.** 80, 547-549, 2002.

9. S. Noda, M. Imada, M. Okano, S. Ogawa, M. Mochizuki and A. Chutinan, " Semiconductor three-dimensional and two-dimensional photonic crystals and devices," *IEEE Journal of Quantum Electronics*, **Vol.** 38, 726-735, 2002.

10. W. Bogaerts, V. Wiaux, D. Taillaert, S. Beckx, B. Luyssaert, P. Bienstman and R. Baets, "Fabrication of photonic crystals in sillion-on-insulator using 248-nm deep UV lithography," *IEEE Journal of Selected Topics in quantum Electronics*, **Vol.** 8, 928-934, 2002.

11. H.-B. Sun, S. Matsuo and H. Misawa, "Three-dimensional photonic crystal structures achieved with two-photon-absorption photopolymerization of resin," *Applied Physics Letters*, **Vol.** 74, 786-788, 1999.

12. M. Campbell, D. N. Sharp, M. T. Harrison, R. G. Denning and A. J. Turberfield, "Fabrication of photonic crystals for the visible spectrum by holographic lithography," *Nature*, **Vol.** 404, 53-56, 2000.

13. T. Kondo, S. Matsuo, S. Juodkazis and H. Misawa, "Femtosecond laser interference technique with diffractive beam splitter for fabrication of three-dimensional photonic crystals," *Applied Physics Letters*, **Vol.** 79, 725-727, 2001.

14. I. B. Divliansky, A. Shishido, I-C. Khoo, D. Pena, S. Nishimura, C.D. Keating, and T. E. Mallouk, "Fabrication of two-dimensional photonic crystals using interference lithography and electrodeposition of CdSe," *Applied physics Letters,* **Vol.** 79, 3392-3394, 2001.

15. I. Divliansky and T.S. Mayer, K. S. Holliday and V. H. Crespi, "Fabrication of three-dimensional polymer photonic crystal structures using single diffraction element

interference lithography," *Applied physics Letters*, **Vol.** 82, 1667-1669, 2003.

16. X. Wang, J .F. Xu, H. M. Su, Z. H. Zeng, Y. L. Chen and H. Z. Wang, "Three-dimensional photonic crystals fabricated by visible light holographic lithography," *Applied physics Letters*, **Vol.** 82, 2212-2214, 2003.

ILLUSTRATIONS

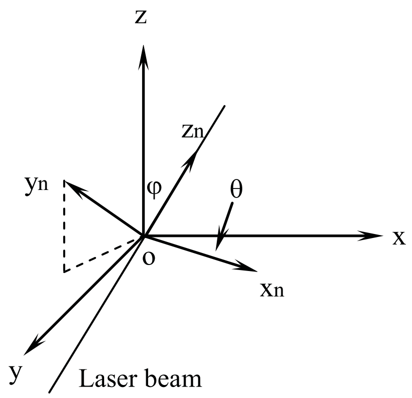

Fig.1 Diagram showing an individual coordinate system of a laser beam and a global coordinate system

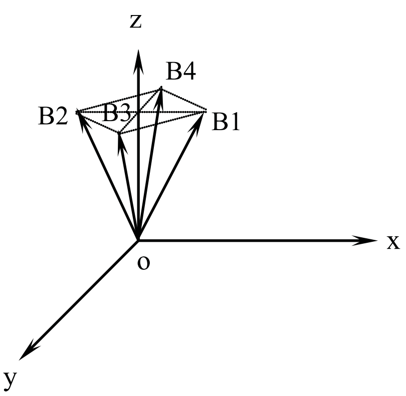

Fig.2 Four-beam interference configuration for producing 2D square structures

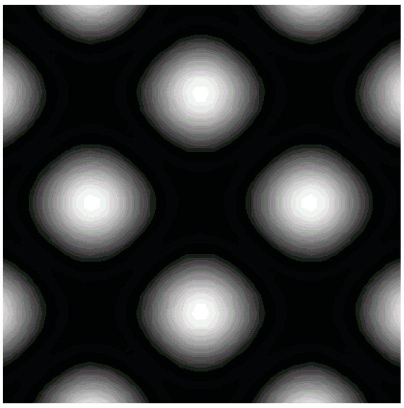

Fig.3 Intensity distribution produced by the four-beam interference configuration shown in Fig.2. All beams linearly polarize in the x-z plane with no phase shift

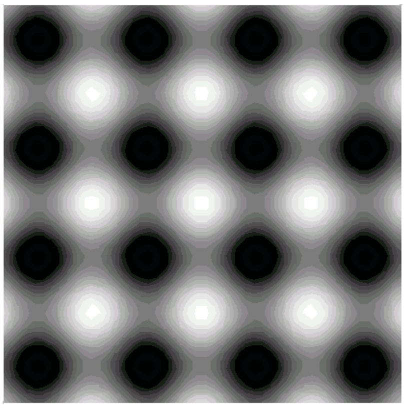

Fig.4 Intensity distribution produced by the four-beam interference configuration shown in Fig.2. B1, B2 linearly polarize in the x-z plane, and B3, B4 linearly polarize in the y-z plane with no phase shift

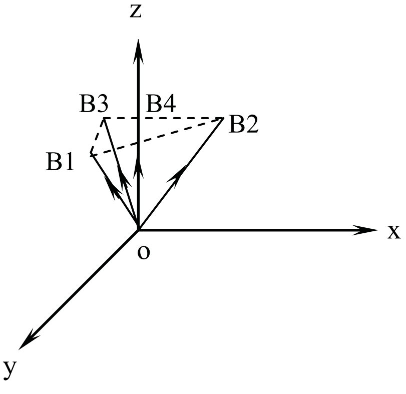

Fig.5 Four-beam interference configuration for producing 3D structures

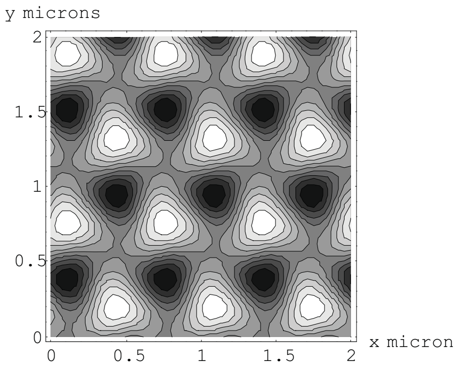

Fig.6 Interference pattern formed in the x-y plane (z=0) in the four beams configuration shown in Fig.5

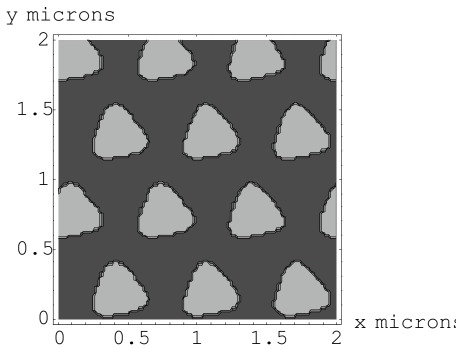

Fig.7 Structure formed when a photoresist exposed to the pattern shown in Fig.6. The dark color indicates the air voids after the photoresist is developed.

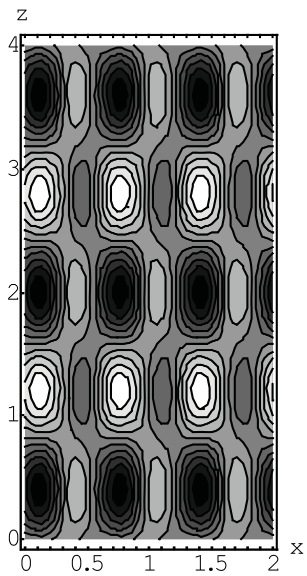

Fig.8 Interference pattern formed in the x-z plane (y=0) in the four-beam configuration shown in Fig.5. Units are microns

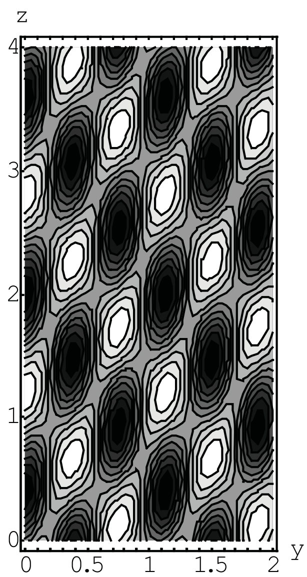

Fig.9 Interference pattern formed in the y-z plane (x=0) in the four-beam configuration shown in Fig.5. Units are microns

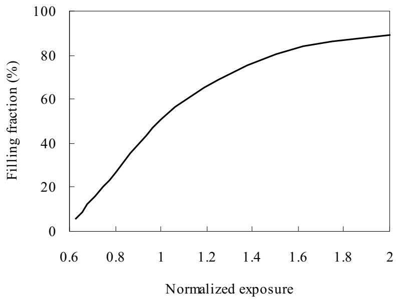

Fig.10 Calculated filling fractions under different exposures

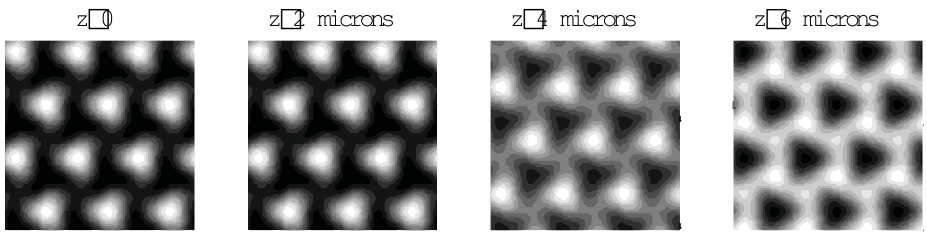

Fig.11 Intensity distributions in the x-y plane at z = 0, 2, 4 and 6 microns when all of the four beams are circularly polarized and B4 has an intensity twice of that of other beams. The scales are 2 microns in both directions

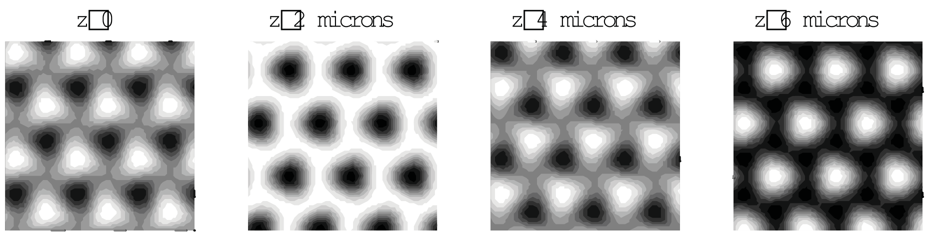

Fig.12 Intensity distributions in the x-y plane at z = 0, 2, 4 and 6 microns when B1, B2 and B3 are linearly polarized, and B4 is circularly polarized. B4 has an intensity twice of that of other beams. The scales are 2 microns in both directions

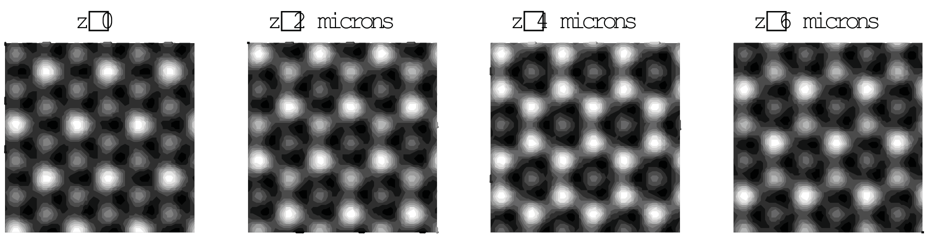

Fig.13 Intensity distributions in the x-y plane at z = 0, 2, 4 and 6 microns when all of the four beams are circularly polarized and B4 has an intensity half of that of other beams. The scales are 2 microns in both directions